Metalloenediynes: Ligand Field Control of Thermal Bergman Cyclization Reactions

ARTICLE *in* JOURNAL OF THE AMERICAN CHEMICAL SOCIETY · JULY 2000

Impact Factor: 12.11 · DOI: 10.1021/ja0017918

3 AUTHORS, INCLUDING:

Diwan S Rawat
University of Delhi
124 PUBLICATIONS **1,643** CITATIONS

Metalloenediynes: Ligand Field Control of Thermal Bergman Cyclization Reactions

Pedro J. Benites, Diwan S. Rawat, and Jeffrey M. Zaleski*

Contribution from the Department of Chemistry, Indiana University, Bloomington, Indiana 47405

Received May 23, 2000

Abstract: We report the preparation and thermal reactivities of unique Cu(I) and Cu(II) metalloenediyne complexes of the flexible 1,8-bis(pyridine-3-oxy)oct-4-ene-2,6-diyne ligand (bpod, **1**). The thermal reactivities of these metalloenediynes are intimately modulated by metal oxidation state. Using differential scanning calorimetry (DSC), we demonstrate that the $[Cu(bpod)_2]^+$ complex (**2**) undergoes Bergman cyclization at 203 °C, whereas the Cu(II) analogue (**3**) is substantially more reactive and cyclizes at 121 °C. Similar results are also observed for mixed ligand $[Cu(bpod)(pyridine)_2]^{+/2+}$ analogues **4** (194 °C) and **5** (116 °C), suggesting that both complexes of a given oxidation state have comparable structures. The $Cu(bpod)Cl_2$ compound (**6**) exhibits a cyclization temperature (152 °C) midway between the those of Cu(I) and Cu(II) complexes, which can be explained by the propensity for *cis*-CuN_2Cl_2 structures to exhibit dihedral angle distortion. The oxidation-state-dependent thermal reactivity is unprecedented and reflects the influence of the ligand field geometry on the barrier to enediyne cyclization. On the basis of X-ray structures of $Cu(pyridine)_4^+$ complexes, **2** and **4** are proposed to be tetrahedral. In contrast, the electronic absorption spectra of **3** and **5** each show a broad envelope that can be Gaussian resolved into three ligand field transitions characteristic of a Cu(II) center in a tetragonal-octahedral environment. This structural assignment is confirmed by the EPR spin Hamiltonian parameters ($g_{\|}/A_{\|}$ (cm) = 134 (**3**), 138 (**5**)) and is consistent with crystallographically characterized $Cu(pyridine)_4X_2$ structures. Molecular mechanics calculations have independently derived comparable tetrahedral and tetragonal structures for **2** and **3**, respectively, and determined the average alkyne termini separation to be $\langle a \rangle = 4.0$ Å for **2** and 3.6 Å for **3**. Thus, the tetrahedral geometries of the copper centers in **2** and **4** increase the distance between alkyne termini relative to the tetragonal Cu(II) geometries of **3** and **5**, and are therefore responsible for the increase in the thermal cyclization temperatures. The DSC and spectroscopic data for **6** support these conclusions, as the latter suggests a distorted four-coordinate structure in the solid state, and a six-coordinate geometry in solution, which gives rise to an intermediate Bergman cyclization temperature. Overall, our results emphasize the utility of newly emerging metalloenediyne complexes for controlling thermal Bergman cyclization reactions and provide insights into designing novel, pharmacologically useful metalloenediyne compounds.

Introduction

The unique diyn-3-ene functionality[1−6] which is behind the DNA-cleaving reactivities of the enediyne antitumor antibiotics has spawned considerable interest in studying the activation and cyclization mechanisms of the natural products for potential pharmaceutical applications.[7] It is now established that the activities of the natural products derives from Bergman cyclization of the enediyne unit which yields a reactive 1,4-benzenoid diradical intermediate[8] that performs H-atom abstraction from the ribose ring of the DNA backbone.[7,9−21]

* To whom correspondence should be addressed. E-mail: zaleski@indiana.edu.

(1) Lee, M. D.; Dunne, T. S.; Siegal, M. M.; Chang, C. C.; Morton, G. O.; Borders, D. B. *J. Am. Chem. Soc.* **1987**, *109*, 3464.
(2) Lee, M. D.; Dunne, T. S.; Chang, C. C.; Ellestad, G. A.; Siegal, M. M.; Morton, G. O.; McGahren, W. J.; Borders, D. B. *J. Am. Chem. Soc.* **1987**, *109*, 3466.
(3) Lee, M. D.; Dunne, T. S.; Chang, C. C.; Siegal, M. M.; Morton, G. O.; Ellestad, G. A.; McGahren, W. J.; Borders, D. B. *J. Am. Chem. Soc.* **1992**, *114*, 985.
(4) Konishi, M.; Ohkuma, H.; Tsuno, T.; Oki, T.; VanDuyne, G. D.; Clardy, J. *J. Am. Chem. Soc.* **1990**, *112*, 3715.
(5) Golik, J.; Clardy, J.; Dubay, G.; Greoenewold, G.; Kawaguchi, H.; Konishi, M.; Krishnan, B.; Ohkuma, H.; Saitoh, K.; Doyle, T. W. *J. Am. Chem. Soc.* **1987**, *109*, 3461.
(6) Golik, J.; Clardy, J.; Dubay, G.; Greoenewold, G.; Kawaguchi, H.; Konishi, M.; Krishnan, B.; Ohkuma, H.; Saitoh, K.; Doyle, T. W. *J. Am. Chem. Soc.* **1987**, *109*, 3462.
(7) Smith, A. L.; Nicolaou, K. C. *J. Med. Chem.* **1996**, *39*, 2103.
(8) Jones, R.; Bergman, R. G. *J. Am. Chem. Soc.* **1972**, *94*, 660.
(9) Paloma, L. G.; Smith, J. A.; Chazin, W. J.; Nicolaou, K. C. *J. Am. Chem. Soc.* **1994**, *116*, 3697.
(10) Kappen, L. S.; Goldberg, I. H. *Biochemistry* **1983**, *22*, 4872.
(11) Zein, N.; McGahren, W. J.; Morton, G. O.; Ashcroft, J.; Ellestead, G. A. *J. Am. Chem. Soc.* **1989**, *111*, 6888.
(12) De Voss, J. J.; Townsend, C. A.; Ding, W.-D.; Morton, G. O.; Ellestad, G. A.; Zein, N.; Tabor, A. B.; Schreiber, S. L. *J. Am. Chem. Soc.* **1990**, *112*, 9669.
(13) Hangeland, J. J.; Voss, J. J. D.; Heath, J. A.; Townsend, C. A.; Ding, W.-D.; Ashcroft, J. S.; Ellestad, G. A. *J. Am. Chem. Soc.* **1992**, *114*, 9200.
(14) Dedon, P.; Salzberg, A. A.; Xu, J. *Biochemistry* **1993**, *32*, 3617.
(15) Christner, D. F.; Frank, B. L.; Kozarich, J. W.; Stubbe, J.; Golik, J.; Doyle, T. W.; Rosenberg, I. E.; Krishnan, B. *J. Am. Chem. Soc.* **1992**, *114*, 8763.
(16) Sugiura, Y.; Shiraki, T.; Konishi, M.; Oki, T. *Proc. Natl. Acad. Sci. U.S.A.* **1990**, *87*, 3831.
(17) Shiraki, T.; Uesugi, M.; Sugiura, Y. *Biochem. Biophys. Res. Commun.* **1992**, *188*, 584.
(18) Shiraki, T.; Sugiura, Y. *Biochemistry* **1990**, *29*, 9795.
(19) Sugiura, Y.; Arakawa, T.; Uesugi, M.; Shiraki, T.; Ohkuma, H.; Konishi, M. *Biochemistry* **1991**, *30*, 2989.
(20) Matsumoto, T.; Okuno, Y.; Sugiura, Y. *Biochem. Biophys. Res. Commun.* **1993**, *195*, 659.
(21) Xu, Y.; Zhen, Y.; Goldberg, I. H. *Biochemistry* **1994**, *33*, 5947.

10.1021/ja0017918 CCC: $19.00
Published on Web 07/14/2000

Since the discovery of the enediynes, through experimental and theoretical examination of the natural products and synthetic analogues researchers have attempted to systematically define the key geometric and electronic factors that affect Bergman cyclization reactivity.[22−45] Early investigations of synthetic carbocyclic enediynes revealed that the rate of Bergman cyclization is dependent upon the distance (*a*) between the terminal alkyne carbons, with 3.4 Å representing the maximum separation allowed for thermal enediyne cyclization at modest temperatures.[24,46] However, detailed theoretical analyses of the reaction coordinate have shown that the relationship between *a* and the activation energy for Bergman cyclization is not exclusive.[47−50] Rather, differential molecular strain in the ground and transition states also contributes significantly to the thermal barrier to enediyne cyclization for carbocyclic enediyne systems. In these cases, direct correlation between *a* and the activation energy for enediyne cyclization does not hold. This notwithstanding, density functional calculations also suggest that if structural perturbations were to reduce *a* to 2.9−3.4 Å, cyclization should occur spontaneously.[51] The theoretical predictions are realized experimentally as there are no documented examples of spontaneous enediyne cyclization for large values of *a* (>3.7 Å) and similarly, no examples of stable enediynes with *a* < 3.1 Å. Thus, although *a* is not the sole contributor to the activation energy for enediyne cyclization, it influences and coarsely correlates with the temperature at which enediynes cyclize for systems without significant molecular strain contributions to the activation barrier.

Scheme 1. Synthesis of 1,8-Bis(pyridine-3-oxy)oct-4-ene-2,6-diyne by Nucleophilic S_N2 Substitution

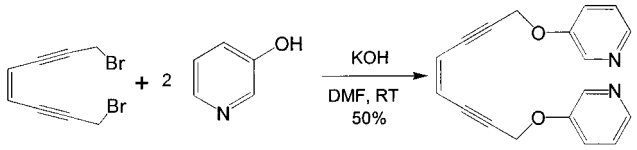

1

The relationships between alkyne termini separation, molecular strain, and Bergman cyclization temperature have been extensively examined for cyclic enediyne systems with 9−12 atoms, but the roles of these parameters have not been as thoroughly studied for larger, more flexible enediyne ring systems (>12 atoms). In these cases, relief of steric encumbrances of the strongly cooperative 9−12-membered ring systems may be expected to diminish the contribution of molecular strain to the temperature for Bergman cyclization. Here, the inherent flexibility of the ring should allow the molecule to adopt conformations that position the alkynes in close proximity during progression to the transition state for Bergman cyclization. The ability to influence the resting enediyne structure, and hence the probability that larger enediyne ring system can acquire the idealized geometry required for Bergman cyclization, is an important criterion for controlling enediyne reactivity.

The recent discovery that enediyne cyclizations can be promoted at reduced temperatures by addition of metal salts has brought to light the utility of transition metals for influencing Bergman cyclization reactions.[52−56] Although it is now clearly established that metal binding can enhance as well as inhibit the reactivity of bound enediyne ligands, systematic correlations of temperature with metal center geometry are sparse.[56] To this end, we have modified the recent synthesis of an enediyne-substituted bipyridine[53] to prepare the flexible 1,8-bis(pyridine-3-oxy)oct-4-ene-2,6-diyne ligand (bpod, **1**) in which the pyridine rings are now tethered solely by the enediyne linkage (Scheme 1). The structural variation allows **1** the flexibility to adopt geometric structures mandated by the d^n electronic configuration of the metal center. The propensity for Cu(II) to be square planar or tetragonal and Cu(I) to be tetrahedral makes these d^9 and d^{10} systems, respectively, ideal candidates for determining if variations in the ligand field geometry about the metal center, induced by changes in oxidation state, could modulate the temperature for Bergman cyclization of the enediyne unit by influencing the distance between the alkyne termini. Herein we report the syntheses, thermal reactivities, and structural evalu-

(22) Takahashi, T.; Tanaka, H.; Yamada, H.; Matsumoto, T.; Sugiura, Y. *Angew. Chem., Int. Ed. Engl.* **1996**, *35*, 1835.
(23) Nicolaou, K. C.; Smith, A. L.; Wenderborn, S. V.; Hwang, C.-K. *J. Am. Chem. Soc.* **1991**, *113*, 3106.
(24) Nicolaou, K. C.; Dai, W.-M. *Angew. Chem., Int. Ed. Engl.* **1991**, *30*, 1387.
(25) Nicolaou, K. C.; Zuccarello, G.; Riemer, C.; Estevez, V. A.; Dai, W.-M. *J. Am. Chem. Soc.* **1992**, *114*, 7360.
(26) Nicolaou, K. C.; Liu, A.; Zeng, Z.; McComb, S. *J. Am. Chem. Soc.* **1992**, *114*, 9279.
(27) Nicolaou, K. C.; Dai, W.-M.; Wendeborn, S. V.; Smith, A. L.; Torisawa, Y.; Maligres, P.; Hwang, C.-K. *Angew. Chem., Int. Ed. Engl.* **1991**, *30*, 1032.
(28) Nicolaou, K. C.; Dai, W.-M.; Tsay, S.-C.; Estevez, V. A.; Wrasidlo, W. *Science* **1992**, *256*, 1172.
(29) Nicolaou, K. C.; Smith, B. M.; Ajito, K.; Komatsu, H.; Gomez-Paloma, L.; Tor, Y. *J. Am. Chem. Soc.* **1996**, *118*, 2303.
(30) Nicolaou, K. C.; Li, T.; Nakada, M.; Hummel, C. W.; Hiatt, A.; Wrasidlo, W. *Angew. Chem., Int. Ed. Engl.* **1994**, *33*, 183.
(31) Zein, N.; Sinha, A. M.; McGahren, W. J.; Ellestad, G. A. *Science* **1988**, *240*, 1198.
(32) Aiyar, J.; Danishefsky, S. J.; Crothers, D. M. *J. Am. Chem. Soc.* **1992**, *114*, 7552.
(33) Aiyar, J.; Hitchcock, S. A.; Denhart, D.; Liu, K. K. C.; Danishefsky, S. J.; Crothers, D. M. *Angew. Chem., Int. Ed. Engl.* **1994**, *33*, 855.
(34) Drak, J.; Iwasawa, N.; Danishefsky, S.; Crothers, D. M. *Proc. Natl. Acad. Sci. U.S.A.* **1991**, *88*, 7464.
(35) Depew, K. M.; Zeman, S. M.; Boyer, S. H.; Denhart, D. J.; Ikemoto, N.; Danishefsky, S. J.; Crothers, D. M. *Angew. Chem., Int. Ed. Engl.* **1996**, *35*, 2797.
(36) Nicolaou, K. C.; Tsay, S.-C.; Suzuki, T.; Joyce, G. F. *J. Am. Chem. Soc.* **1992**, *114*, 7555.
(37) Nicolaou, K. C.; Smith, A. L. *Acc. Chem. Res.* **1992**, *25*, 497.
(38) Li, H.; Zeng, Z.; Estevez, V. A.; Baldenius, K. U.; Nicolaou, K. C.; Joyce, G. F. *J. Am. Chem. Soc.* **1994**, *116*, 3709.
(39) Liu, C.; Smith, B. M.; Ajito, K.; Komatsu, H.; Gomez-Paloma, L.; Li, T.; Theodorakis, E. A.; Nicolaou, K. C.; Vogt, P. K. *Proc. Natl. Acad. Sci. U.S.A.* **1996**, *93*, 940.
(40) Ho, S. N.; Boyer, S. H.; Schreiber, S. L.; Danishefsky, S. J.; Crabtree, R. G. *Proc. Natl. Acad. Sci. U.S.A.* **1994**, *91*, 9203.
(41) Shair, M. D.; Yoon, T.; Chou, T. C.; Danishefsky, S. J. *Angew. Chem., Int. Ed. Engl.* **1994**, *33*, 2477.
(42) Myers, A. G.; Fraley, M. E.; Tom, N. J.; Cohen, S. B.; Madar, D. J. *Chem., Biol.* **1995**, *2*, 33.
(43) Myers, A. G.; Cohen, S. B.; Tom, N. J.; Madar, D. J.; Fraley, M. E. *J. Am. Chem. Soc.* **1995**, *117*, 7574.
(44) Elbaum, D.; Porco, J. A., Jr.; Stout, T. J.; Clardy, J.; Schreiber, S. L. *J. Am. Chem. Soc.* **1995**, *117*, 211.
(45) Chatterjee, M.; Mah, S. C.; Tullius, T. D.; Townsend, C. A. *J. Am. Chem. Soc.* **1995**, *117*, 8074.
(46) Nicolaou, K. C.; Smith, A. L.; Yue, E. W. *Proc. Natl. Acad. Sci. U.S.A.* **1993**, *90*, 5881.
(47) Magnus, P.; Lewis, R. T.; Huffman, J. C. *J. Am. Chem. Soc.* **1988**, *110*, 6921.
(48) Magnus, P.; Fortt, S.; Pitterna, T.; Snyder, J. P. *J. Am. Chem. Soc.* **1990**, *112*, 4986.
(49) Snyder, J. P. *J. Am. Chem. Soc.* **1989**, *111*, 7630.
(50) Snyder, J. P. *J. Am. Chem. Soc.* **1990**, *112*, 5367.
(51) Schreiner, P. R. *J. Am. Chem. Soc.* **1998**, *120*, 4184.
(52) Warner, B. P.; Millar, S. P.; Broene, R. D.; Buchwald, S. L. *Science* **1995**, *269*, 814.
(53) Konig, B.; Pitsch, W.; Thondorf, I. *J. Org. Chem.* **1996**, *61*, 4258.
(54) Basak, A.; Shain, J. A. *Tetrahedron Lett.* **1998**, *39*, 3029.
(55) Basak, A.; Shain, J. *Tetrahedron Lett.* **1998**, *39*, 1623.
(56) Coalter, N.; Concolino, T. E.; Streib, W. E.; Hughes, C. G.; Rheingold, A. L.; Zaleski, J. M. *J. Am. Chem. Soc.* **2000**, *122*, 3112.

ations of novel copper metalloenediynes of **1** that exhibit large variations in Bergman cyclization temperatures based on metal complex oxidation state and hence geometry.

Experimental Section

Materials. All preparations were carried out in an inert atmosphere (nitrogen) using Schlenk and drybox techniques. Hydrocarbon solvents such as ether, benzene, and tetrahydrofuran were dried by distillation over sodium/benzophenone. Acetonitrile, dichloromethane, dimethyl sulfoxide, and *n*-butylamine were dried and distilled from calcium hydride. Benzene, tetrahydrofuran, dichloromethane, and dimethyl sulfoxide were stored over 4-Å molecular sieves. NMR solvents (acetonitrile-d_3, dimethyl sulfoxide-d_6, and chloroform-d_3) were dried over activated 3- and 4-Å molecular sieves and degassed by bubbling with nitrogen for 30 min. Deuterated solvents for air-sensitive metal complexes were purchased in sealed ampules (under nitrogen), dried with molecular sieves, and degassed. Degassed spectroscopic grade solvents were used for all UV−vis and EPR measurements.

Chemicals. All chemicals used in the synthesis of the copper metalloenediynes were of the highest purity available from Aldrich and Fluka and were used as received. The organic enediyne compounds were purified by flash chromatography with 60-Å silica gel (430−230 μm) using HPLC grade hexanes, ethyl acetate, dichloromethane, and methanol.

Physical Measurements. Electron paramagnetic resonance spectra were recorded on an ESP 300 Bruker instrument under the following conditions: microwave frequency, ∼9.5 GHz; microwave power, 10−20 mW; modulation amplitude, 3−10 G; modulation frequency, 100 kHz; receiver gain, $(2.5-5) \times 10^4$. Electronic spectra were obtained on a Perkin-Elmer Lambda 19 UV/vis/NIR spectrometer. For the ligand field UV−vis measurements, the error in the energies is 5 cm^{-1} at 13 500 cm^{-1}. ^1H and ^{13}C NMR spectra were recorded on a 300-MHz Varian Gemini-2000 NMR spectrometer, using the residual proton resonance of the solvent as an internal reference. The multiplicity of the ^{13}C signals was determined by the DEPT technique and quoted as (+) for CH_3 or CH, (−) for CH_2, and (C_{quat}) for quaternary carbons. High-resolution DCI, EI, and FAB MS spectra were acquired on a Kratos MS-80 mass spectrometer that was interfaced with a Kratos DS90 data system. ESI MS data were obtained at the University of Illinois with a Micromass Quattro I mass spectrometer. Infrared (KBr pellet or neat) spectra were recorded on a Nicolet 510P FT-IR spectrometer, and elemental analyses of the samples were obtained from Atlantic Microlab, Inc. Differential scanning calorimetry (DSC) traces were recorded on a General V4.1C DuPont 910 DSC differential scanning calorimeter coupled to a Dupont Thermal Analyst 2100 at a heating rate of 10 °C min^{-1}.

Molecular Modeling. Molecular mechanics calculations at the MMX force field level were performed using the PCModel v.7.0 (Serena Software), on a Silicon Graphics O2R5000 Unix workstation.

Synthesis of 1,8-Bis(tetrahydropyran-2-yloxy)oct-4-ene-2,6-diyne. To a mixture of $(PPh_3)_4Pd$ (1.1 g, 0.95 mmol), CuI (1.1 g, 5.8 mmol), and *n*-butylamine (34.2 g, 468.2 mmol) in anhydrous benzene (150 mL) was added tetrahydro-2-(2-propynyloxy)-2*H*-pyran (11.1 g, 79.3 mmol) dropwise by an addition funnel at 0 °C in 10 min. The reaction mixture was allowed to warm and was stirred at room temperature for 20 min. The flask was then cooled to 0 °C, and *cis*-dichloroethylene (3.8 g, 39.6 mmol) was added by syringe under N_2. The mixture was stirred for 8 h at 40 °C. Solvent was removed in vacuo, and cold hexanes was added to precipitate the inorganic material. The solution was filtered through a bed of silica gel, and the solvent was removed from the filtrate. The residue was chromatographed (flash chromatography) on silica gel (10% ethyl acetate/hexanes): yield, 9.5 g (78%); viscous oil; $R_f = 0.14$; ^1H NMR (300 MHz, $CDCl_3$) δ (ppm) 5.81 (s, 2H), 4.83 (t, 2H), 4.41 (d, 4H), 3.83 (m 2H), 3.51 (m, 2H), 1.76 (m, 4H), 1.54 (m, 8H); ^{13}C NMR (300 MHz, $CDCl_3$) δ (ppm) 119.3 (+), 96.6 (+), 92.9 (C_{quat}), 82.9 (C_{quat}), 61.9 (−), 54.6 (−), 30.2 (−), 25.3 (−), 18.9 (−); IR (neat, cm^{-1}) 2992, 2869, 1029; FAB-MS *m*/*z* 304.17 [M^+, calcd for $C_{18}H_{24}O_4$ 304.17].

Synthesis of 1,8-Dibromooct-4-ene-2,6-diyne. To a solution of PPh_3 (15.9 g, 60.5 mmol) in CH_2Cl_2 (100 mL) was added Br_2 (9.7 g, 60.7 mmol) dropwise at 0 °C under N_2, and a thick orange precipitate formed in solution. The compound 1,8-bis(tetrahydropyran-2-yloxy)oct-4-ene-2,6-diyne (6.1 g, 20.0 mmol) at 0 °C was then added, and the mixture was stirred for 30 min at room temperature. Two-thirds of the solvent was removed by distillation, and the remaining suspension was poured into petroleum ether (PE, 100 mL). The precipitate was filtered and washed with PE (2 × 30 mL), and the combined organic phases were concentrated in vacuo. Flash chromatography (1.5% ethyl acetate/hexanes) gave the compound as a light yellow oil: yield, 3.94 g (75%); $R_f = 0.15$; ^1H NMR (300 MHz, $CDCl_3$) δ (ppm) 5.88 (s, 2H), 4.11 (s, 4H); ^{13}C NMR (300 MHz, $CDCl_3$) δ (ppm) 120.1 (+), 92.2 (C_{quat}), 83.4 (C_{quat}), 14.8 (−); IR (neat, cm^{-1}) 3435, 2993, 2912, 2184, 2167, 2093, 1994, 1660, 1576, 1439, 1408, 1311, 1228, 1057, 954, 933, 700; HR-MS (EI) *m*/*z* 264/262 [M^+], 181/183 [$M^+ - Br$], 102 [$M^+ - 2Br$].

Synthesis of 1,8-Bis(pyridine-3-oxy)oct-4-ene-2,6-diyne (bpod, 1). A mixture of 3-hydroxypyridine (1.0 g, 10.5 mmol) and KOH (6.0 g,107 mmol) in 10 mL of DMF was stirred for 30 min. To this solution was the added rapidly 1,8-dibromooct-4-ene-2,6-diyne (1.4 g, 5.4 mmol) in 5 mL of DMF while the temperature was maintained at 20 °C. The reaction mixture was filtered after 15 min, and the compound was extracted by CH_2Cl_2. The organic phase was dried over $MgSO_4$ and evaporated in vacuo. Flash chromatography (4% MeOH/CH_2Cl_2) gave the compound as a pale yellow oil: yield, 0.78 g (50%); $R_f = 0.21$; ^1H NMR (300 MHz, $CDCl_3$) δ (ppm) 8.40 (d, 2H), 8.20 (d, 2H), 7.24−7.30 (m, 4H), 5.90 (s, 2H), 5.89 (s, 4H); ^{13}C NMR (300 MHz, $CDCl_3$) δ (ppm) 153.7 (C_{quat}), 142.8 (+), 138.6 (+), 123.8 (+), 121.9 (+), 119.8 (+), 90.9 (C_{quat}), 84.6 (C_{quat}), 56.7 (−); IR (neat, cm^{-1}) 3056, 3038, 2934, 2867, 2733, 2633, 2585, 2498, 2216, 2010, 1892, 1817, 1722, 1686, 1576, 1475, 1427, 1375, 1332, 1275, 1228, 1180, 1159 1130, 1103, 1074, 1049, 1001, 798, 706, 619, 542, 415; HR-MS (EI) *m*/*z* 290.105 [M^+, calcd for $C_{18}H_{14}N_2O_2$ 290.141].

Synthesis of $[Cu(bpod)_2]PF_6$ (2). A 50-mL Schlenk flask was charged with 44.7 mg (0.12 mmol) of $[Cu(CH_3CN)_4]PF_6$, which was then dissolved in 2.5 mL of degassed acetonitrile. A degassed solution of compound **1**, 81.2 mg (0.28 mmol), in 2.5 mL of acetonitrile was slowly added by cannula, and the mixture was stirred at 40 °C under nitrogen for 12 h. Concentration of the resulting solution and addition of 10 mL of diethyl ether resulted in the precipitation of a pale yellow solid, which was filtered, washed with diethyl ether, and dried under vacuum: yield, 66.2 mg (70%); mp 305 °C dec; ^1H NMR (300 MHz, DMSO-d_6) δ (ppm) 8.19−8.31 (m, 8H), 7.21−7.40 (m, 8H), 5.97 (s, 4H), 4.92 (s, 8H); ^{13}C NMR (300 MHz, DMSO-d_6) δ (ppm) 153.8 (C_{quat}), 142.8 (+), 138.4 (+), 124.5 (+), 122.1 (+), 120.6 (+), 92.4 (C_{quat}), 84.8 (C_{quat}), 56.8 (−); IR (KBr, cm^{-1}) 3550, 3063, 2939, 2218, 2095, 1576, 1479, 1437, 1277, 1230, 999, 844, 691; ESI MS (electrospray mass spectrometry) *m*/*z* 643.2/645.3 $^{63,65}Cu$ [M^+, calcd for $C_{36}H_{28}N_4O_4Cu$ 643.1/645.1]. Anal. Calcd for $C_{36}H_{28}N_4O_4CuPF_6$: C, 54.81; H, 3.55; N, 7.11. Found: C, 54.98; H, 3.68; N, 6.83.

Synthesis of $[Cu(bpod)_2](NO_3)_2$ (3). A flask was charged with 69.6 mg (0.30 mmol) of $Cu(NO_3)_2 \cdot 2.5H_2O$, which was then dissolved in 2.5 mL of methanol. A solution of 174.0 mg (0.60 mmol) of compound **1** in 2.5 mL of methanol was slowly added, and the solution was stirred at room temperature for 12 h. Concentration of the resulting solution and addition of 20 mL of diethyl ether resulted in the precipitation of a bright green solid, which was washed with diethyl ether and dried in vacuo. The compound was recrystallized from a 1:4 solution of methanol and diethyl ether: yield, 170.63 mg (65%); mp 356 °C dec; IR (KBr, cm^{-1}) 3400, 3063, 2939, 2218, 2090, 1576, 1484, 1437, 1384, 1280, 1232, 994, 806, 698; ESI MS (electrospray mass spectrometry) *m*/*z* 643.3/645.2 $^{63,65}Cu$ [M^+, calcd for $C_{36}H_{28}N_4O_4Cu$ 643.1/645.1]. Anal. Calcd for $C_{36}H_{28}N_6O_{10}Cu \cdot 3.5H_2O$: C, 52.04; H, 4.22; N, 10.12. Found: C, 52.35; H, 4.17; N, 9.92.

Synthesis of $[(Cu(bpod)(py)_2]PF_6$ (4). A 50-mL round-bottom Schlenk flask was charged with 200 mg (0.69 mmol) of compound **1**, which was then dissolved in 15 mL of dry degassed acetonitrile. To the solution 223 mg (0.60 mmol) of $[Cu(CH_3CN)_4]PF_6$ was added, and the mixture was allowed to stir for 2 h. Then 94.6 mg (1.2 mmol) of dry degassed pyridine was added, and the reaction mixture was allowed to stir overnight. The solvent was removed under vacuum, and the compound was allowed to dry for 2 h. To the dark yellow solid diethyl ether was added, and the compound was allowed to stir for 1 h. The

Scheme 2. Metal Complexation Reactions for the Preparation of Copper Metalloenediynes **2** and **3**

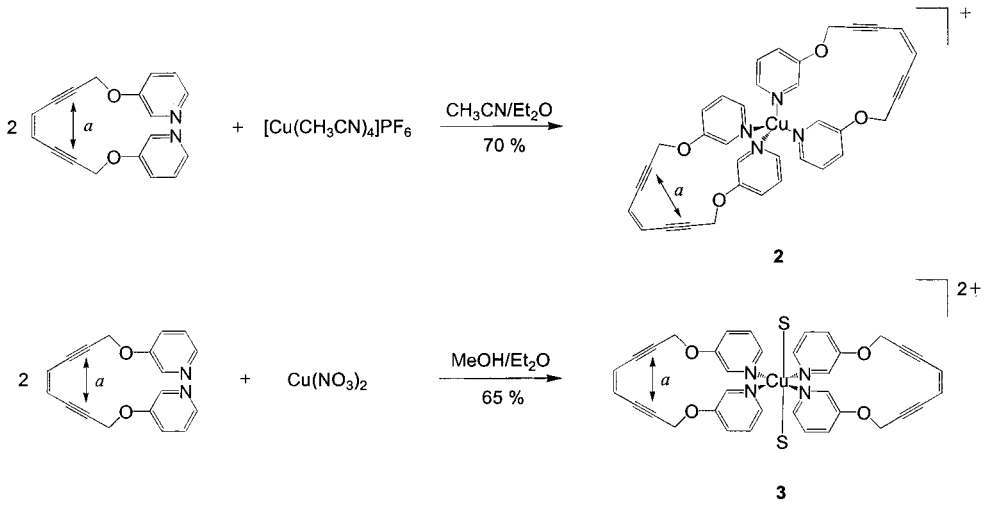

compound was filtered under anaerobic conditions and dried under vacuum to yield a dark yellow solid: yield, 200 mg (51%); mp 242 °C dec; ^{1}H NMR (300 MHz, CD_3CN) δ (ppm) 8.51 (d, 4H), 8.25 (d, 2H), 8.18 (d, 2H), 7.81 (m, 2H), 7.31−7.41 (m, 8H), 5.95 (s, 2H), 4.91 (s, 4H); ^{13}C NMR (300 MHz, CD_3CN) δ (ppm) 154.9 (C_{quat}), 150.6 (+), 143.7 (+), 138.8 (+), 137.6 (+), 125.4 (+),125.2 (+), 123.5 (+),120.7 (+), 92.1 (C_{quat}), 85.1 (C_{quat}), 57.4 (−); IR (KBr, cm^{-1}) 3063, 2964, 2505, 2217, 1574, 1482, 1442, 1277, 1229, 998, 842, 700. Anal. Calcd for $C_{28}H_{24}N_4O_2CuPF_6$: C, 51.22; H, 3.66; N, 8.54. Found: C, 51.24; H, 3.85; N, 8.42.

Synthesis of [Cu(bpod)(py)$_2$](NO$_3$)$_2$ (5). A 150-mL round-bottom flask was charged with 128.6 mg (0.66 mmol) of $Cu(py)_2Cl_2$,[57] which was then dissolved in 50 mL of reagent grade acetonitrile. The solution was heated to 45 °C overnight with a condenser to dissolve the compound. Then 225.3 mg (1.33 mmol) of $AgNO_3$ was added, and the solution was stirred for 3 h. The white precipitate formed was filtered, and the excess solvent from the light blue filtrate was removed. Next, 250 mg (0.86 mmol) of compound **1** was dissolved in 10 mL of acetonitrile and added to the filtrate. The solution was allowed to stir overnight, resulting in a dark green color as the desired complex was formed. The product was filtered and dried overnight under vacuum: yield, 395 mg (93%); mp 128 °C dec; IR (KBr, cm^{-1}) 3421, 3060, 2213, 1575, 1483, 1436, 1384, 1279, 1232, 995, 805, 698; ESI MS (electrospray mass spectrometry) *m*/*z* 636.3/638.0 ^{63,65}Cu [M$^+$, calcd for $C_{28}H_{24}N_4O_2Cu\cdot 2NO_3$ 636/638], 415.1/417.1. Anal. Calcd for $C_{28}H_{24}N_6O_8Cu\cdot 2H_2O$: C, 50.07; H, 3.57; N, 12.51. Found: C, 50.39; H, 3.82; N, 12.68.

Synthesis of Cu(bpod)Cl$_2$ (6). A 50-mL round-bottom flask was charged with 60 mg (0.35 mmol) of $CuCl_2\cdot 2H_2O$, which was then dissolved in 5 mL of reagent grade methanol. A 102 mg (0.35 mmol) amount of **1** was dissolved in 5 mL of methanol and added dropwise to the round-bottom flask, and the solution was stirred overnight to give a bright blue-green precipitate. The solid product was filtered and dried under vacuum overnight: yield 111.8 mg (76%); mp 225 °C dec; IR (KBr, cm^{-1}) 3057, 2217, 1603, 1574, 1477, 1437, 1276, 1229, 1001, 809, 690; ESI MS (electrospray mass spectrometry) *m*/*z* 388.1/390.1 ^{63,65}Cu [M$^+$ − Cl, calcd for $C_{18}H_{14}N_2O_2CuCl$ 389.3/391.3]. Anal. Calcd for $C_{18}H_{14}N_2O_2CuCl_2$: C, 50.89; H, 3.32; N, 6.59. Found: C, 50.56; H, 3.35; N, 6.61.

Characterization of Thermal Product (7) Derived from 2. A sealed NMR tube under nitrogen was charged with **2** and a 2-fold excess of 1,4-cyclohexadiene in 600 μL of DMSO-d_6. The mixture was allowed to react as the temperature was raised from 25 °C to 90 °C in 1 h increments. The reaction was monitered by ^{1}H NMR, which revealed exclusive conversion to **7** after 8 h ($t_{1/2}$ = 5.3 h). One-half of the deuterated solvent was distilled in vacuo to remove the volatile hydrogen donor, and the compound was redissolved in DMSO-d_6: ^{1}H NMR (300 MHz, DMSO-d_6) δ (ppm) 8.39−8.54 (m, 8H), 7.57 (m, 4H), 7.68 (m, 4H), 7.39−7.42 (m, 8H), 5.40 (s, 8H); ^{13}C NMR (300 MHz, DMSO-d_6) δ (ppm) 156.0 (C_{quat}), 143.5 (+), 139.6 (+), 136.4 (C_{quat}), 130.3 (+), 129.9 (+), 125.6 (+), 122.9 (+), 68.9 (−); ESI MS (electrospray mass spectrometry) *m*/*z* 647.2/649.1 ^{63,65}Cu [M$^+$, calcd for $C_{36}H_{32}N_4O_4Cu$ 647.3/649.2].

Characterization of Thermal Product (8) Derived from 3. A round-bottom flask was charged with 50 mg of **3**, and a 100-fold excess of 1,4-cyclohexadiene was added in 5 mL of methanol. The mixture was heated to 60 °C overnight. The light green solution turned to dark green upon heating. The solvent was removed under vacuum, and upon addition of diethyl ether, a dark brown-green solid was formed. The solid was washed with methanol and diethyl ether and dried overnight under vacuum. The solid was then dissolved in reagent grade dimethylformamide. Excess EDTA (10-fold) was added, and the solution was allowed to cool overnight until a solid precipitate formed. The precipitate was filtered, and the filtrate was kept to extract the organic thermal product after removal of copper ions by EDTA. The organic product was extracted with methylene chloride and washed with water using a separating funnel. The organic layer was dried with $MgSO_4$ and the solvent removed in vacuo. A dark brown oil was obtained and purified by flash chromatography (20% MeOH/CH_2Cl_2): yield, 20 mg (88%); R_f = 0.47; ^{1}H NMR (300 MHz, $CDCl_3$) δ (ppm) 8.36 (d, 2H), 8.22 (d, 2H), 7.51 (m, 2H), 7.41 (m, 2H), 7.21−7.25 (m, 4H), 5.21 (s, 4H); ^{13}C NMR (300 MHz, $CDCl_3$) δ (ppm) 155.0 (C_{quat}), 142.9 (+), 138.5 (+), 134.8 (C_{quat}), 129.7 (+), 129.3 (+), 124.4 (+), 121.1 (+), 68.7 (−); HR-MS (EI) *m*/*z* 292.15 [M$^+$, calcd for $C_{18}H_{16}N_2O_2$ 292.14].

Results and Discussion

Syntheses. The enediyne ligand 1,8-bis(pyridine-3-oxy)oct-4-ene-2,6-diyne (bpod, **1**) was prepared by deprotonation of 2 equiv of 3-hydroxypyridine with KOH and subsequent nucleophilic attack at the terminal carbons of 1,8-dibromooct-4-ene-2,6-diyne (Scheme 1). The resulting product was washed extensively with water and extracted with CH_2Cl_2. Compound **1** was then dried and purified by flash chromatography. The structure of compound **1** was confirmed by ^{1}H and ^{13}C NMR and mass spectrometry.

The Cu(I) complex ([Cu(bpod)$_2$]PF$_6$, **2**) was prepared by reacting 2:1 molar equivalents of **1** with $[Cu(CH_3CN)_4]PF_6$ in acetonitrile under nitrogen (Scheme 2). The compound was precipitated by addition of ether to yield **2** (70%) as a yellow solid. The [Cu(bpod)$_2$](NO$_3$)$_2$ complex (**3**) was synthsized by a similar approach using 1 equiv of $Cu(NO_3)_2\cdot 2.5H_2O$ and 2 equiv of the enediyne ligand **1** to yield **3** (65%) as a light green powder. The mixed Cu(I) complex ([Cu(bpod)(py)$_2$]PF$_6$ **4**) was prepared by addition of 1 equiv of **1** to $[Cu(CH_3CN)_4]PF_6$ to

(57) Gill, N. S.; Nyholm, R. S.; Barclay, G. A.; Christie, T. I.; Pauling, P. J. *J. Inorg. Nucl. Chem.* **1961**, *18*, 88.

Scheme 3. Preparation of Mixed Ligand Copper Metalloenediynes **4**−**6**

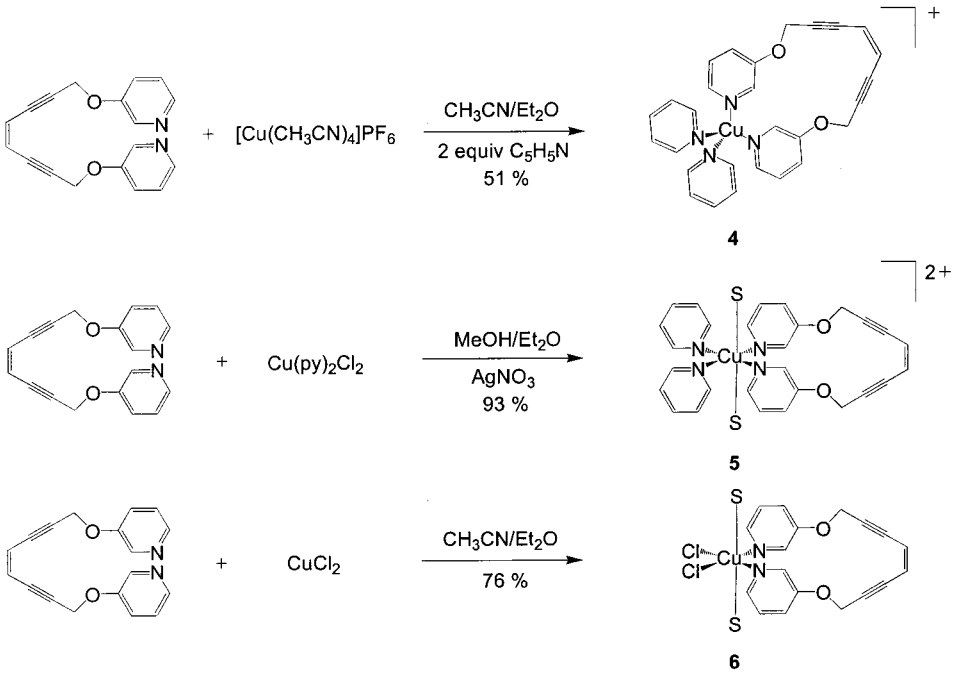

Scheme 4. Thermal Cyclization Reaction of **2** and **3** To Yield Products **7** and **8**

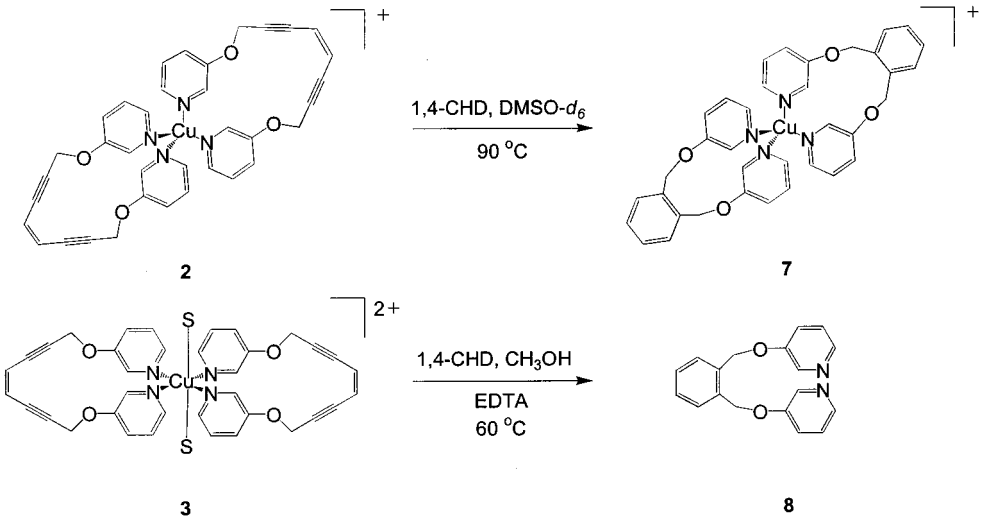

yield the Cu(I) monoenediyne complex in situ prior to the addition of 2 equiv of pyridine (Scheme 3). The Cu(II) analogue ($[Cu(bpod)(py)_2](NO_3)_2$, **5**) was synthesized from the corresponding $Cu(py)_2Cl_2$ starting material by precipitation of the chlorides with $AgNO_3$. The analogous neutral compound Cu(bpod)Cl_2 (**6**) was obtained by reacting **1** with $CuCl_2$ in a 1:1 stoichiometry in methanol, followed by repeated washings with ether. The identities of these copper metalloenediynes were confirmed by ^{1}H and ^{13}C (DEPT) NMR (for **2** and **4**), elemental analyses, and mass spectrometry.

Thermal Reactivity. The thermal cyclizations of **1**−**3** were initially examined in solution to determine the identity of the thermal reaction products. In a sealed NMR tube compound **1** was heated in DMSO-d_6 with a 2-fold excess of cyclohexadiene (CHD) as an H-atom donor. In the absence of copper, no Bergman-cyclized product was detected following heating for 7 h at 90 °C. Our observations are in accordance with the thermal reactivity of 1,2-bis(diphenylphosphinoethynyl)benzene, which is stable when heated at 95 °C for several days in the presence of a hydrogen donor.[52] However, upon being heated to 120 °C for 8 h, the compound readily decomposes under these conditions. The thermal cyclization of **2** was also studied in solution under the same experimental conditions. The Cu(I) complex showed exclusive conversion to the Bergman-cyclized product **7** after being heated at 90 °C for 8 h ($t_{1/2}$ = 5.3 h) (Scheme 4). The progress of the reaction was followed by monitoring the disappearance of the olefinic protons of the enediyne ligands at δ 5.97 ppm and the appearance of two sets of multiplets (4H each) at δ 7.57 and 7.68 ppm, corresponding to a 1,2-disubstituted benzene product bound to Cu(I), as well as a shift in the $-OCH_2$ resonance from δ 4.92 ppm to δ 5.40 ppm. Formation of the 1,6-Bergman-cyclized product was confirmed by ^{13}C (DEPT) NMR, which showed the disappearance of the quaternary alkyne resonances at δ 84.8 and 92.4 ppm, and alkene resonance at δ 120.6 ppm, as well as the appearance of new signals at δ 129.9 and 130.3 ppm corresponding to the C−H carbons of the 1,2-disubstituted benzene ring product. These chemical shift assignments, and those of the remaining carbons, were verified by both comparison with an analogous literature compound[58] and simulation of the ^{13}C

Table 1. Differential Scanning Calorimetry Results for **1**−**6**

compound	cyclization temperature/°C
bpod (**1**)	245[a]
$[Cu(bpod)_2]PF_6$ (**2**)	203
$[Cu(bpod)_2](NO_3)_2$ (**3**)	121
$[Cu(bpod)(py)_2]PF_6$ (**4**)	194
$[Cu(bpod)(py)_2](NO_3)_2$ (**5**)	116
$Cu(bpod)Cl_2$ (**6**)	152

[a] Temperature recorded in the solid state within a matrix of compound **3**. The cyclization temperature for **1** as a neat oil is 136 °C.

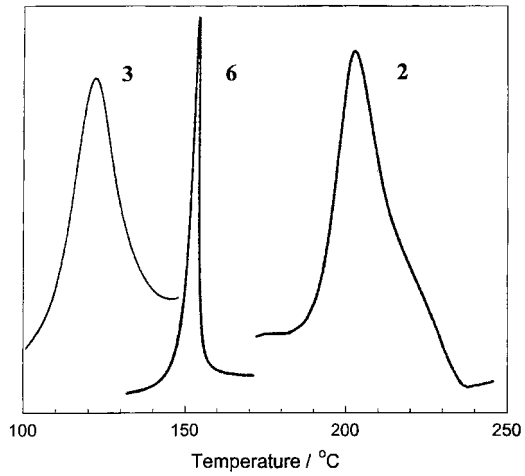

Figure 1. Differential scanning calorimetry traces of compounds **2**, **3**, and **6**.

spectrum of the organic ligand.[59] The same procedures were used to rule out the formation of 1,5- and 2,5-cyclized products which have been reported for radical-mediated cyclization of enediynes.[60] Product identity was also confirmed by mass spectrometry of cyclized Cu(I) product, **7** (m/z = 647). The thermal cyclization of the Cu(II) complex in solution was also examined by heating **3** at 60 °C for 12 h. Due to the paramagnetism of the metal center, the formation of Bergman-cyclized product could be definitively confirmed only by extraction of the metal with EDTA and subsequent characterization of the organic ligand. Like the Cu(I) thermal cyclization reaction, this procedure also yielded the 1,6-Bergman-cyclized ligand product **8**, thereby documenting the ability of the metal center to enhance the reactivity of the enediyne ligand.

In an effort to more clearly evaluate the relative reactivities of enediynes **1**−**6**, the thermal cyclization temperatures for these compounds were measured in the solid state by differential scanning calorimetry (DSC) (Table 1, Figure 1). The free ligand **1** exhibits an exothermic peak at 245 °C corresponding to Bergman cyclization of the enediyne moiety. The temperature compares favorably with those of both the 1,2-bis(diphenylphosphinoethynyl)benzene ligand (243 °C)[52] and the 3,3′-dihydroxybipyridyl analogue (237 °C)[53] previously reported. In contrast to the high thermal barrier for **1** in the solid state, complexes **2**−**6** each posesses a single exergonic feature at markedly reduced temperatures. For the bis(enediyne) complexes **2** and **3**, the cyclization temperatures are separated by 82 °C (**2**, 203 °C; **3**, 121 °C). Although these values are in the same range as those reported for metal-assisted thermal cyclizations of chelating enediyne ligands by metal salts,[52,53] their cyclization temperatures are intimately mediated by the oxidation state of the copper centers. The same trend is confirmed for the mixed ligand Cu(I) and Cu(II) compounds **4** and **5**, which have two ancillary pyridines in place of one chelating enediyne. These complexes show cyclization temperatures nearly identical to those of **2** and **3** (**4**, 194 °C; **5**, 116 °C), respectively, despite the considerable difference in their molecular topologies and, presumably, in their solid state packing. In general, we find that this parameter does not strongly influence the solid-state cyclization temperatures for these compounds, as 1:1 mixtures of, for example, **2** and **3** or **1** and **2** reveal cyclization temperatures for the individual components that vary by <5 °C from those of the pure species. Finally, the cyclization temperature for **6** in the solid state lies between those for the Cu(I) (**2**, **4**) and Cu(II) complexes (**3**, **5**) with N_4 coordination. This behavior can be ascribed to geometric structural differences between N_4 and N_2Cl_2 inner-sphere coordination to copper (vide infra).

Table 2. Ligand Field Absorption Band Energies for Cu(II) complexes of **1**

compound	ligand field band energies/cm^{-1}	
	solid	solution
$[Cu(bpod)_2](NO_3)_2$ (**3**)	16 983, 15 424, 13 972	14 203, 12 732, 11 471
$[Cu(bpod)(py)_2](NO_3)_2$ (**5**)	17 517, 15 731, 14 103	15 493, 13 779, 12 132
$Cu(bpod)Cl_2$ (**6**)	16 559, 14 731, 13 110	12 321, 10 465, 8533

Table 3. EPR Parameters for Cu(II) complexes of **1**

compound	$g_{\|\|}$	$g_\perp$	$A_{\|\|} \times 10^{-4}$ cm^{-1}	$g_{\|\|}/A_{\|\|}$ (cm)
$[Cu(bpod)_2](NO_3)_2$ (**3**)	2.27	2.05	169	134
$[Cu(bpod)(py)_2](NO_3)_2$ (**5**)	2.21	1.98	160	138
$Cu(bpod)Cl_2$ (**6**)	2.24	1.99	146	153

Structure Evaluation. We have also evaluated the structures of **2**−**6** using a combination of spectroscopic (Tables 2 and 3) and computational methods. On the basis of the structures of analogous tetrakispyridine copper(I) complexes and simple ligand field theory arguments, the Cu(I) complexes **2** and **4** would be expected to possess tetrahedral geometry with a dihedral angle near 90°.[61] The ^1H and ^{13}C NMR spectra of these complexes reveal two equivalent enediyne or pyridyl ligands, indicating a symmetric copper center in solution. In contrast, Cu(II) complexes with an N_4 ligand field can adopt coordination numbers from 4 to 6, the latter via solvent or counterion ligation,[62] and have geometries ranging from square planar[63,64] to *cis*[65,66] or *trans*[67−72] distorted octahedral. A combination of electronic absorption spectroscopy in the ligand field region and

(58) Ouchi, A.; Koga, Y. *J. Org. Chem.* **1997**, *62*, 7376.
(59) (a) ChemWindow 3, v.3.1, Softshell International. (b) H, C NMR Spectrum Generator 3.5, ACD/Labs Software, Toronto, ON, Canada.
(60) Ramkumar, D.; Kalpana, M.; Varghese, B.; Sankararaman, S.; Jagadeesh, M. N.; Chandrasekhar, J. *J. Org. Chem.* **1996**, *61*, 2247.
(61) Nilsson, K.; Oskarsson, A. *Acta Chem. Scand. Ser. A.* **1982**, *36*, 605.
(62) Addison, A. W.; Carpenter, M.; Lau, L. K.-M.; Wicholas, M. *Inorg. Chem.* **1978**, *17*, 1545.
(63) Chan, C.-W.; Mingos, D. M. P.; White, A. J. P.; Williams, D. J. *Polyhedron* **1996**, *15*, 1753.
(64) Koning, C. E.; Challa, G.; Hulstergen, F. B.; Reedijk, J. *J. Mol. Catal.* **1986**, *34*, 355.
(65) Fitzgerald, W.; Murphy, B.; Tyagi, S.; Walsh, B.; Walsh, A.; Hathaway, B. *J. Chem. Soc., Dalton Trans.* **1981**, 2271.
(66) Fereday, R. J.; Hodgson, P.; Tyagi, S.; Hathaway, B. J. *J. Chem. Soc., Dalton Trans.* **1981**, 2070.
(67) Haynes, J. S.; Rettig, S. J.; Sams, J. R.; Trotter, J.; Thompson, R. C. *Inorg. Chem.* **1988**, *27*, 1237.
(68) Beurskens, G.; Martens, C. F.; Nolte, R. J. M.; Beurskens, P. T.; Smits, J. M. M. *J. Chem. Cryst.* **1995**, *25*, 425.
(69) Agnus, Y.; Labarelle, M.; Louis, R.; Metz, B. *Acta Crystallogr., Sect. C (Cryst. Struct. Commun.)* **1994**, *50*, 536.

EPR have proven very effective for characterizing the structures of Cu(II) centers in both inorganic complexes[73−75] and protein active sites.[76,77] Typically, four-coordinate square planar complexes exhibit three optical absorption features ($^2B_{1g} \rightarrow {}^2A_{1g}$, $^2B_{1g} \rightarrow {}^2B_{2g}$, $^2B_{1g} \rightarrow {}^2E_g$ in D_{4h}) between 17 000 and 20 000 cm^{-1}, whereas for six-coordinate tetragonal structures this envelope is shifted to lower energy (11 000−16 000 cm^{-1}). Both of these geometries are readily distinguished from pseudotetrahedral structures for a given ligand set as the latter typically exhibit d−d bands between 5000 and 14 000 cm^{-1}, depending upon the strength of the specific ligand field and the degree of compression of the tetrahedron toward the square plane.[78] The weaker the ligand field, and the greater the distortion toward the tetrahedron, the lower the transition energies.

The electronic absorption spectrum of **3** in solution exhibits a broad envelope with $\lambda_{max} = 770$ nm (12 987 cm^{-1}/MeOH, Figure 2a) that can be Gaussian resolved into three ligand field transitions centered at 11 471, 12 732, and 14 203 cm^{-1}, characteristic of a Cu(II) center in a tetragonal-octahedral environment. The bathochromatic shift of the absorption maximum upon dissolution of **3** in the stronger coordinating solvent DMSO ($\lambda_{max} = 820$ nm)[62] also suggests inner-sphere solvent coordination (S in Scheme 2). In the solid state, the optical bands shift to higher energy by ∼2500−2700 cm^{-1}, but the envelope remains centered at relatively low energy (∼15 400 cm^1), in keeping with a six-coordinate structure in the solid state derived from nitrate or water coordination.

The EPR spectrum of **3** (Figure 2b) reveals that the Cu(II) center is indeed axial ($g_{\|} > g_{\perp} > 2.0$), with simulated spin Hamiltonian parameters $g_{\|} = 2.27$, $g_{\perp} = 2.05$, and $A_{\|} = 169 \times 10^{-4}$ cm^{-1}. These values lie in the middle of the Peisach/Blumberg maps[79] and most closely correlate with copper in the 2+ oxidation state in tetragonal CuN_4X_2 structures ($g_{\|} \approx 2.25$, $A_{\|} \approx (150-250) \times 10^{-4}$ cm^{-1}).[73,75,80,81] Moreover, the appearance of weak pyridine nitrogen superhyperfine splitting of the $g_{\perp}$ component (nine-line pattern, $A_N = 15.6$ G) is consistent with four equivalent nitrogen atoms in a nearly planar arrangement. The ratio $g_{\|}/A_{\|}$ is small (134 cm), demonstrating the absence of significant dihedral angle distortion in the *xy*-plane. In addition, the optical and EPR data for **3** correlate very well with crystallographically characterized tetrakispyridine complexes of Cu(II).[67−72] Based on the above chemical and spectroscopic evidence, the structures of **2** and **3** are best described as four-coordinate tetrahedral and six-coordinate tetragonal Cu(I) and Cu(II) complexes, respectively.

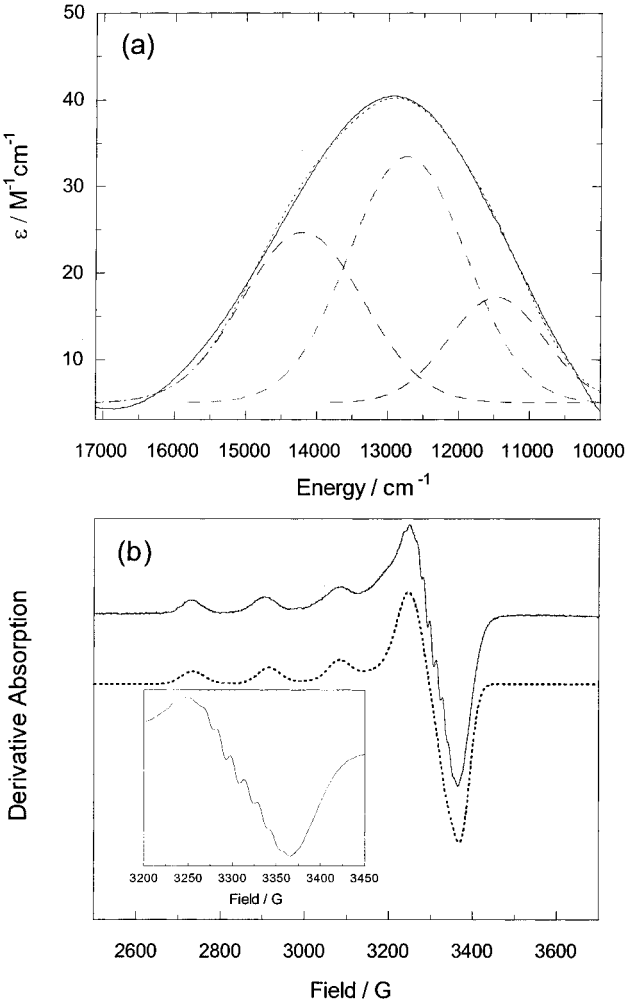

Figure 2. (a) Ligand field region electronic absorption spectrum of **2** in MeOH at 293 K. The experimental spectrum (—) can be fit by three Gaussian band shapes (- - -) centered at 14 203, 12 732, and 11 471 cm^{-1} and is plotted against the resultant sum (•••) of these components. (b) Observed (—) and calculated (•••) X-band EPR spectrum of **3** in MeOH at 77 K. The $g_{\perp}$ region is expanded (inset) to illustrate the nine-line superhyperfine splitting pattern arising from four pyridyl nitrogens in the *xy*-plane ($A_N = 15.6$ G). Simulated EPR parameters including $^{63}Cu/^{65}Cu$ isotopic distribution: $g_{\|} = 2.27$, $g_{\perp} = 2.05$, $A_{\|} = 169 \times 10^{-4}$ cm^{-1}.

Using these features as a basis, the electronic absorption and EPR spectra for the Cu(II) complexes **5** and **6** (Figures 3 and 4) have also been measured to compare the structures of these metalloenediynes to that of **3**. As expected, **5** exhibits electronic absorption spectra comparable (Figure 3a, Table 2) to those of **3** with small shifts (600−1300 cm^{-1}) in the d−d transition maxima to higher energy. In the solid state, the optical transitions for **5** are shifted to higher energy relative to those in solution by ∼2000 cm^{-1}. These shifts are nearly identical to those observed for **3**. The absorption maximum at ∼15 700 cm^{-1} is also consistent with a weak six-coordinate tetragonal environment in the solid state. The EPR spectrum of **5** in solution (Figure 3b) is axial with $g_{\|} = 2.21$, $g_{\perp} = 1.98$, and $A_{\|} = 160 \times 10^{-4}$ cm^{-1}. Once again, analysis of the second-derivative spectrum reveals a nine-line superhyperfine splitting pattern from the four equatorial nitrogens of the pyridyl rings ($A_N = 13.9$ G). Moreover, the ratio $g_{\|}/A_{\|}$ is also small (138 cm), consistent with a nearly planar arrangement of the tetrapyridyl ligand field. Together, these results support a tetragonal six-coordinate environment about the Cu(II) center in **5**, both in

(70) Zhang, W.; Jeitler, J. R.; Turnbull, M. M.; Landee, C. P.; Wei, M.; Willett, R. D. *Inorg. Chem. Acta* **1997**, *256*, 183.
(71) Holzbock, J.; Sawodny, W.; Walz, L. *Z. Kristallogr.* **1997**, *212*, 115.
(72) Durand, P. B.; Holt, E. M. *Acta Crystallogr., Sect C. (Cryst. Struct. Commun.)* **1995**, *51*, 850.
(73) Comba, P.; Hambley, T. W.; Hitchman, M. A.; Stratemeier, H. *Inorg. Chem.* **1995**, *34*, 3903.
(74) Batra, G.; Mathur, P. *Inorg. Chem.* **1992**, *31*, 1575.
(75) Uma, R.; Viswanathan, R.; Palaniandavar, M.; Lakshminarayanan, M. *J. Chem. Soc., Dalton Trans.* **1994**, 1219.
(76) Peisach, J. Pulsed EPR Studies of Copper Proteins. In *Bioinorganic Chemistry of Copper*; Karlin, K., Tyeklar, Z., Eds.; Chapman and Hall: New York, 1993; p 21.
(77) Solomon, E. I.; Sundaram, U. M.; Machonkin, T. E. *Chem. Rev.* **1996**, *96*, 2563.
(78) Lever, A. B. P. *Inorganic Electronic Spectroscopy*, 2nd ed.; Elsevier: Amsterdam, 1984.
(79) Peisach, J.; Blumberg, W. E. *Arch. Biochem. Biophys.* **1974**, *165*, 691.
(80) Davis, W. M.; Zask, A.; Nakanishi, K.; Lippard, S. J. *Inorg. Chem.* **1985**, *24*, 3737.
(81) Pradilla, S. J.; Chen, H. W.; Koknat, F. W.; Fackler, J. P. *Inorg. Chem.* **1979**, *18*, 3519.

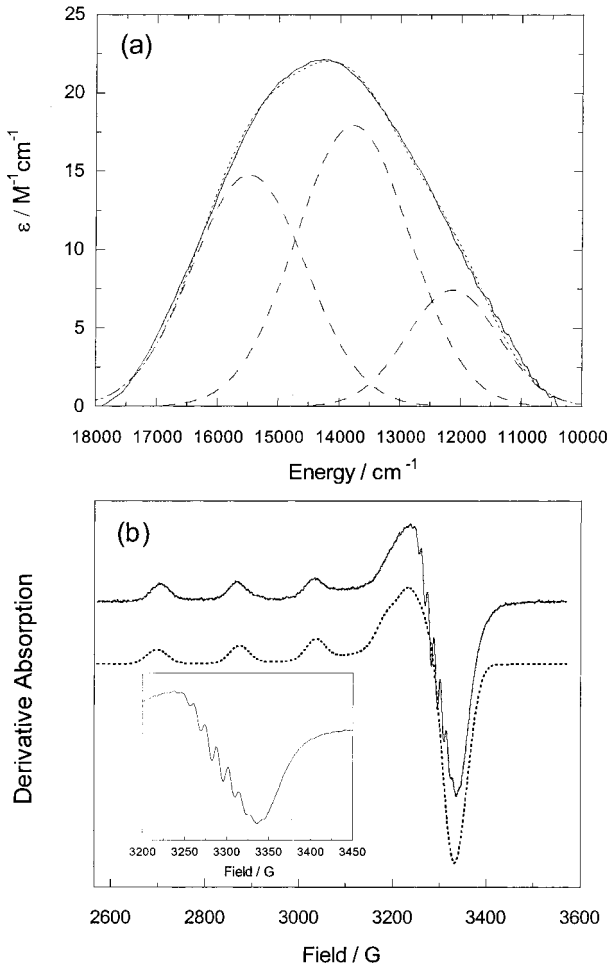

Figure 3. (a) Electronic absorption spectrum (d−d bands) of **5** in MeOH at 293 K. The experimental absorption profile (—) can be fit by three Gaussian band shapes (- - -) centered at 15 493, 13 779, and 12 132 cm^{-1} and is plotted against the resultant sum (•••) of these components. (b) Observed (—) and calculated (•••) X-band EPR spectrum of **5** in MeOH at 77 K. The $g_\perp$ region is expanded (inset) to illustrate the nine-line superhyperfine splitting pattern arising from four pyridyl nitrogens in the *xy*-plane (A_N = 13.9 G). Simulated EPR parameters including $^{63}Cu/^{65}Cu$ isotopic distribution: $g_\parallel = 2.21$, $g_\perp = 1.98$, $A_\parallel = 160 \times 10^{-4}$ cm^{-1}.

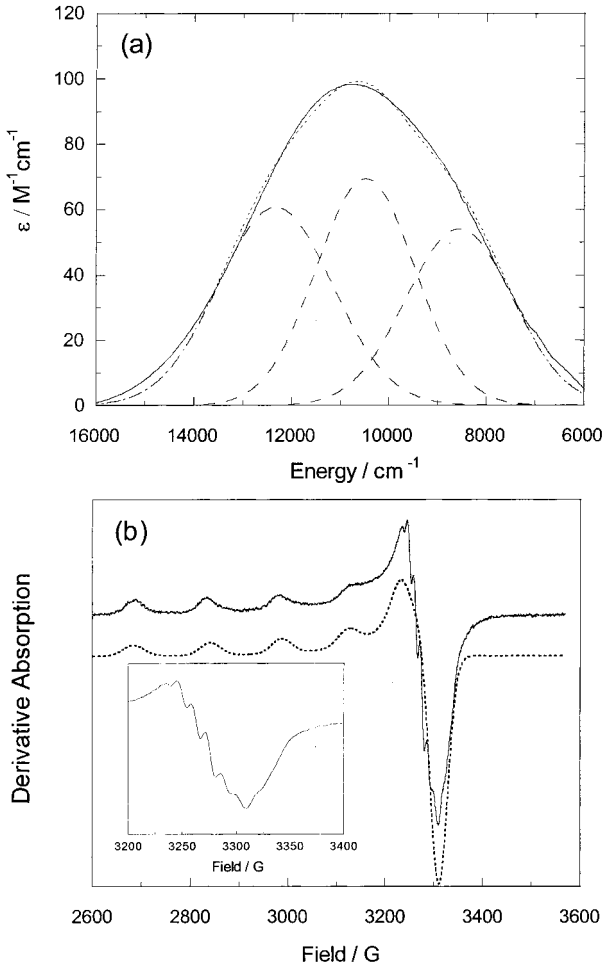

Figure 4. (a) Ligand field region electronic absorption spectrum of **6** in DMSO at 293 K. The experimental spectrum (—) can be fit by three Gaussian band shapes (- - -) centered at 12 321, 10 465, and 8533 cm^{-1} and is plotted against the resultant sum (•••) of these components. (b) Observed (—) and calculated (•••) X-band EPR spectrum of **6** in 4:1 MeOH/DMSO at 77 K. The $g_\perp$ region is expanded (inset) to illustrate the five-line superhyperfine splitting pattern arising from two pyridyl nitrogens in the *xy*-plane (A_N = 13.4 G). Simulated EPR parameters including $^{63}Cu/^{65}Cu$ isotopic distribution: $g_\parallel = 2.24$, $g_\perp = 1.99$, $A_\parallel = 146 \times 10^{-4}$ cm^{-1}.

the solid state and in solution. The correspondence in the spectroscopic features for **3** and **5** suggests that the metal center geometries in these complexes are very similar, thereby leading to comparable Bergman cyclization temperatures for these Cu(II) complexes.

The electronic absorption and EPR spectra of **3** and **5** correlate well with structural trends developed for CuN_4X_2 systems. However, introduction of Cl^- into the ligand field can strongly influence the observed spectral features due to the strong σ- and π-donation from the p-orbitals of the chloride to the metal d-manifold.[82] For *cis*-CuN_2Cl_2 complexes, the net structural effect is dihedral angle distortion that can range from 0 to 90°, where ~80% of the known structures exhibit weakly distorted to tetrahedral geometries.[83] However, of the *cis*-CuN_2Cl_2 structures, only one in five structures are actually tetrahedral, indicating that these complexes most commonly have distortion angles ranging from $10° \leq \theta \leq 70°$. The spectral ramifications are generally two-fold, namely a reduction in the λ_{max} for the electronic absorption profile[78] and the potential for chloride ($I = {}^3/_2$) superhyperfine coupling in the EPR spectrum.[82,84]

The electronic absorption and EPR spectra for **6** (Figure 4) are strongly influenced by the N_2Cl_2 coordination sphere. In general, the electronic absorption bands in solution (DMSO, Figure 4a) are centered very low in energy (~10 400 cm^{-1}). In DMF, the absorption profile maximum shifts to higher energy by 960 cm^{-1}, indicating that solvent is coordinated to the Cu(II) center in solution. Typically, four-coordinate *cis*-CuN_2Cl_2 structures with pseudotetrahedral geometries exhibit absorption maxima between 11 000 and 14 000 cm^{-1},[84] which is in the same range expected for six-coordinate $CuN_2Cl_2X_2$ complexes. Due to the solvent dependence of the absorption maximum and the low energy of the profile, the best structural representation of **6** in solution is a six-coordinate species with two solvent molecules bound axially with a modest dihedral distortion of the *xy*-plane. The EPR spectrum of **6** (Figure 4b) is consistent with this type of structure, as an axial signal is observed with $g_\parallel = 2.24$, $g_\perp = 1.99$, and $A_\parallel = 146 \times 10^{-4}$

(82) Solomon, E. I. *Comments Inorg. Chem.* **1984**, *3*, 225.

(83) The statistics for CuN_2Cl_2 structures were obtained from examination of 46 *cis* and 28 *trans* entries in Cambridge Structure Database which could be unambiguously identified with the desired structural class.

(84) Kokoszka, G. F.; Reimann, C. W.; H. C. Allen, J. *J. Phys. Chem.* **1967**, *71*, 121.

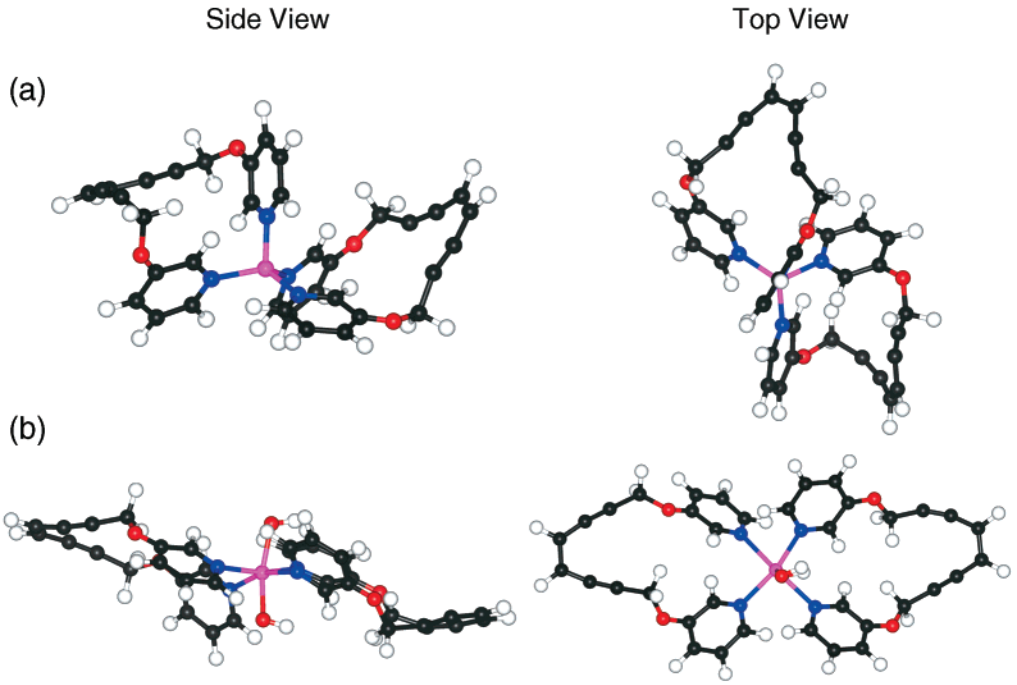

Figure 5. Geometric structures of copper metalloenediynes (a) **2** ($\langle a \rangle$ = 4.0 Å) and (b) **3** ($\langle a \rangle$ = 3.6 Å) determined by molecular mechanics/dynamics calculations at the MMX force field level. Atom color designations: copper, pink; nitrogen, blue; oxygen, red; carbon, black; and hydrogen, white.

cm^{-1}. A second-derivative analysis of the spectrum reveals a prominent five-line superhyperfine splitting pattern from two equivalent nitrogens with a coupling constant very similar to those of **3** and **5** (A_N = 13.4 G). In addition, the ratio $g_{||}/A_{||}$ is 153 cm, suggesting an intermediate degree of dihedral distortion of the N_2Cl_2 plane. These conclusions are supported by the EPR parameters of tetrahedral Cu(phen)Cl_2, for which $A_{||} = 123 \times 10^{-4}$ cm^{-1} and $g_{||}/A_{||}$ = 187 cm.[84]

Interestingly, the absorption maximum for **6** in the solid state is shifted to higher energy by ~4400 cm^{-1} (14 700 cm^{-1}). Also, elemental analysis of **6** shows no solvent present in the solid material. The pronounced dependence of the absorption maximum coupled with the absence of solvent in the elemental analysis suggests that the compound is four-coordinate in the solid state. However, the absorption profile in the solid state is somewhat lower in energy than expected for a rigidly planar, four-coordinate CuN_2Cl_2 structure (Table 2).[78,82] At the same time, the structure is likely not tetrahedral, as the absorption maximum for such a system would lie between 11 000 and 14 000 cm^{-1}.[82,84] Since $A_{||}$ and $g_{||}/A_{||}$ for **6** in a frozen glass indicate that the structure in solution is a distorted six-coordinate geometry, the structure for **6** in the solid state is best described as a four-coordinate, flattened tetrahedron where the dihedral angle is likely between 20 and 60° based on the spectroscopic data. Since >70% of the *cis*-CuN_2Cl_2 structures in the Cambridge Structure Database exhibit comparable degrees of dihedral distortion, the solid-state structure of **6** derived from the spectroscopic data is consistent with this geometry. The moderate degree of dihedral distortion is also consistent with the solid-state Bergman cyclization temperature for **6**, which is nearly midway between those of tetrahedral (**2** and **4**) and tetragonal (**3** and **5**) Cu(II) geometries.

In an effort to determine the influence of the copper center geometry on the alkyne termini separation, we have performed molecular mechanics calculations at the MMX force field level[85] to evaluate the ground-state structures of **2** and **3**. This method has been used effectively to predict thermal reactivities of metal-assisted Bergman cyclization reactions through determination of the distance between alkyne termini.[52] Within this theme, we have now calculated 60 possible structures for four-, five-, and six-coordinate copper metalloenediyne complexes using direct energy minimization. Several of the lowest energy structures were then used as starting points for molecular dynamics simulations to determine the ground-state structures of **2** and **3** at ambient temperature. The protocol for the dynamics simulations allowed the starting structures to access thermal bath modes at 800 K prior to cooling to a final sample temperature of 300 K. For the Cu(I) complex **2**, as predicted by ligand field theory, tetrahedral geometry of the CuN_4 core is the dominant lowest energy structure and consistently reproduced from all initial geometric starting points (Figure 5). The average alkyne termini separation, $\langle a \rangle$, was then calculated from an ensemble of the five tetrahedral structures lowest in energy. The relative energies of these structures span 8 kcal/mol, with a modest standard deviation in the mean energy of 2.9%. From this structural subset, $\langle a \rangle$ was determined to be 4.0 Å for **2**, which correlates well with the aggressive thermal requirements for cyclization of this complex and the qualitative relationship between distance and cyclization temperature for synthetic enediyne systems.

The same dynamics approach was used in conjunction with the experimental data to assess the structure of the Cu(II) complex **3**. The geometry of **3** was initially modeled as a square plane of CuN_4 coordination with two OH ligands depicting axially bound solvent molecules. The template structure was energy minimized and produced two plausible geometries: one with solvent molecules *cis*, and the other very close to the starting structure with *trans* solvent coordination. In all cases, the lowest energy structures obtained were always of the *trans* configuration. An ensemble of the four lowest energy tetragonal structures (range, 8 kcal/mol; SDEV = 3.1%) yielded an average alkyne termini distance of $\langle a \rangle$ = 3.6 Å. In comparison to the thermal Bergman cyclization reactivities for **2** and **3**, these

(85) PCModel, Serena Software, Bloomington, IN 47405.

results show that the tetrahedral geometry of **2** causes significant distortion of the enediyne unit and forces the alkyne termini to a greater separation distance (0.4 Å) than the less strained tetragonal structure of **3**. Thus, the disposition of the 1,5-diyne-3-ene linkage can be intimately mediated by the geometric requirements of the d^n electronic configuration of the metal, resulting in profound effects upon the thermal reactivity of the metalloenediyne complex. The structure/reactivity correlation for compounds **2** and **3** is conserved in **3**−**6**. The tetrahedral and tetragonal structures of **4** and **5**, respectively, are reflected in the similarties of the Bergman cyclization temperatures of these complexes to those of **2** and **3**, which illustrates the role of the metal geometry in controlling the cyclization temperature of the enediyne ligand. The DSC temperature resulting from the distorted geometry of **6** logically falls between those of the tetrahedral Cu(I) and tetragonal Cu(II) complexes, further confirming the pronounced influence of the metal geometry to systematically modulate the enediyne cyclization temperature.

Conclusion

In conclusion, we have described the preparation of novel Cu(I) and Cu(II) metalloenediyne complexes and shown their thermal reactivities to be strongly influenced by the oxidation state of the metal center, and hence the geometry of the resulting complex. Overall, our correlation between metalloenediyne structure and thermal reactivity demonstrates that enediyne cyclizations can indeed be controlled by judicious choice of metal complex oxidation state and geometry. These results emphasize the utility of newly emerging metalloenediyne complexes for controlling thermal Bergman cyclization reactions and provide insights into potential designs for pharmacologically useful metalloenediyne compounds.

Acknowledgment. We thank Drs. Mark Pagel and Ulrike Werner-Zwanziger of the Indiana University NMR and Molecular Visualization Facilities for technical assistance. The generous support of the American Cancer Society (RPG-99-156-01-C), the donors of the Petroleum Research Fund (PRF No. 33340-G4), administered by the American Chemical Society, and Research Corporation (Research Innovation Award No. RI0102 for J.M.Z) are gratefully acknowledged. P.J.B. and D.S.R contributed equally to this study.

JA0017918